JOURNAL OF MATERIALS SCIENCE 9 (1974) 456–463

An electron microscope study of gadolinium iron garnet thin films prepared by the oxidation of vacuum evaporated metals

A. G. FITZGERALD, T. G. MAY
Carnegie Laboratory of Physics, University of Dundee, Dundee, Scotland

The oxidation of thin films of gadolinium, iron and Gd_3Fe_5 has been investigated by transmission electron microscopy and diffraction between 300 and 1200° C. The oxidation products for gadolinium and iron films are consistent with the oxidation mechanism proposed for bulk material. Thin films of Gd_3Fe_5 do not oxidize completely to give gadolinium iron garnet, high densities of garnet and orthoferrite inclusions are observed. An unusual form of grain growth is also observed in these films.

1. Introduction

Techniques for the growth of thin films of magnetic oxides have been a subject of intensive study in recent years, mainly due to possible applications of these materials, in thin film form, in computers and microwave devices. The preparation techniques which have been studied include sputtering [1], chemical vapour deposition from mixed halide vapours [2], growth from molten solution [3] and vacuum deposition of metals with subsequent oxidation [4]. An extensive bibliography of preparation techniques has been given by Mee *et al* [2].

The present investigation of gadolinium iron garnet thin films prepared by oxidation of the relevant metal thin films stems from the original X-ray diffraction study of Banks *et al* [4]. Their investigation indicated that it may be possible to grow polycrystalline magnetic oxide thin films by this technique. However, until recently [5], the microstructure of such films has not been studied and the possibility of other included oxide phases had not been investigated.

The aims of the present study have been to prepare thin gadolinium iron garnet films by oxidation of vacuum deposited thin films of composition Gd_3Fe_5, to determine the temperature range in which oxidation of the composite metal thin films to garnet occurs free from other oxide phases, and to examine the growth and microstructure of these garnet thin films. The oxidation process has been investigated over the temperature range of 300 to 1200° C and oxide structures have been identified by electron diffraction. The oxidation processes in thin films of iron and gadolinium have also been studied in order to follow the solid state reactions which occur on formation of gadolinium iron garnet thin films.

2. Experimental

Thin films of gadolinium and iron and films of composition Gd_3Fe_5 were prepared by vacuum deposition in a 12 in. coating unit at a pressure of 10^{-6} Torr. The gadolinium source was of 99.9 % purity and the iron source was 99.999 % pure. Evaporation was effected by means of an electron beam source and for Gd_3Fe_5 films, depositions were made without breaking vacuum. The thickness and stoichiometry of the vacuum deposited films were controlled by means of a thickness monitor of the quartz crystal oscillator type. The thicknesses of metal films studied varied between 30 and 50 nm. The films were deposited upon single crystal rock salt substrates or on mica coated with a thin carbon film. The oxidation and sintering studies were made with films which had been detached, by immersion in distilled water, from the mica and rock salt substrates and mounted upon platinum electron

microscope grids. An AEI EM6G electron microscope operated at 100 kV was used to examine the crystal structure and microstructure of the oxidized thin films.

3. Thin-film oxidation

3.1. Oxidized iron and gadolinium thin films

The results of the oxidation of iron in thin film form have been discussed in a previous investigation [5] and appear to contradict observations of the oxidation of iron in bulk. Only below an oxidation temperature of 600°C are the oxidation products of iron in bulk and in thin film form similar, α-Fe_2O_3 with spinel phases are formed. On bulk iron the oxides form a stratified scale upon the surface in the following sequence [6],

$$Fe + Fe_3O_4 + \gamma\text{-}Fe_2O_3 + \alpha\text{-}Fe_2O_3 + \text{oxidizing agent} .$$

Between 600 and 900°C the oxidation products are difficult to identify. Owing to crystallite sizes and randomness of orientations selected-area electron diffraction patterns are not easy to interpret.

Above 900°C single crystal orientations of α-Fe_2O_3 only, are usually observed upon oxidation of thin iron films, although on rare occasions single crystal spinel orientations have been identified. This contrasts with the scale of $FeO + Fe_3O_4 + Fe_2O_3$ which is formed upon iron [6]. These observations, however, are consistent since in a thin film there is not a large reservoir for the formation of iron ions and, therefore, the oxides FeO and Fe_3O_4, which depend for stability upon the diffusion of Fe^{2+} and Fe^{3+} ions [7] will be very rapidly replaced in a thin film by α-Fe_2O_3 formed in contact with the oxidizing atmosphere at the surface. This reaction proceeds by oxygen diffusion via anion vacancies in FeO and Fe_3O_4 until the film is completely oxidized to α-Fe_2O_3.

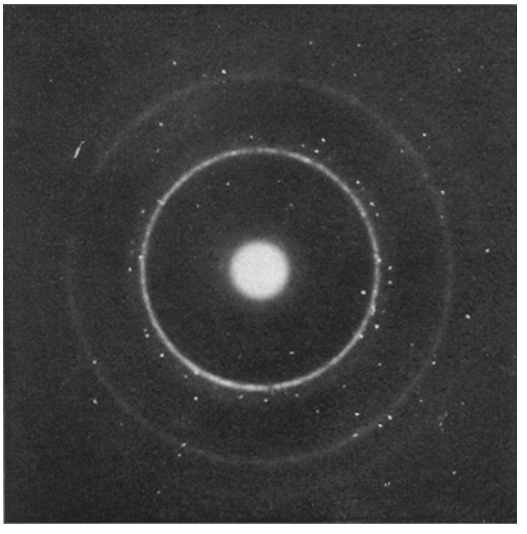

Figure 1 Electron diffraction pattern from a cubic gadolinium sesquioxide film formed by oxidation of a gadolinium film for 12 h at 600°C.

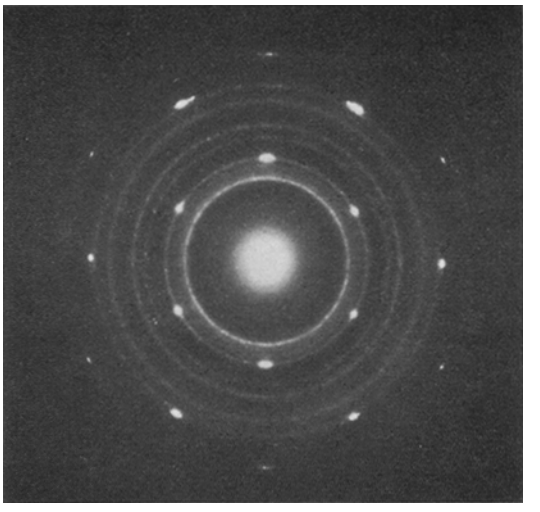

Figure 2 Electron diffraction pattern from a Gd_3Fe_5 film oxidized at 300°C for 10 min. The pattern consists of a single crystal spot pattern due to α-Fe_2O_3 with the electron beam parallel to [0001] and a polycrystalline pattern due to Gd_2O_3.

In contrast to the variety of oxides produced upon oxidation of iron thin films only one oxide, the cubic sesquioxide, Gd_2O_3, is formed upon oxidation of gadolinium thin films within the temperature range 300 to 1000°C. This observation agrees with bulk oxidation studies of gadolinium [8]. Fig. 1 shows a selected-area electron diffraction pattern from a cubic gadolinium sesquioxide thin film formed by oxidation of a gadolinium thin film.

3.2. Oxidation of Gd_3Fe_5 thin films

In the temperature range 300°C to approximately 700°C, selected-area electron diffraction patterns from oxidized films of Gd_3Fe_5 indicate that oriented regions of α-Fe_2O_3 are formed together with areas of Gd_2O_3, in polycrystalline form, agreeing with observations of the oxidation of the individual metal thin films (Fig. 2).

Above an oxidation temperature of approxi-

mately 700°C, a solid state reaction begins to take place and areas of garnet, orthoferrite, cubic rare earth sesquioxide and α-Fe_2O_3 have been identified by selected-area electron diffraction. At oxidation temperatures of greater than 850°C a significant increase in grain size is observed and single crystal orientations of the orthoferrite and garnet crystal structures are observed (Figs. 3 and 4). With increasing oxidation temperature the proportion of orthoferrite decreases, however, for Gd_3Fe_5 films, at oxidation temperatures of as high as 1100°C, included crystallites of gadolinium orthoferrite have been identified in gadolinium iron garnet films (Fig. 3a).

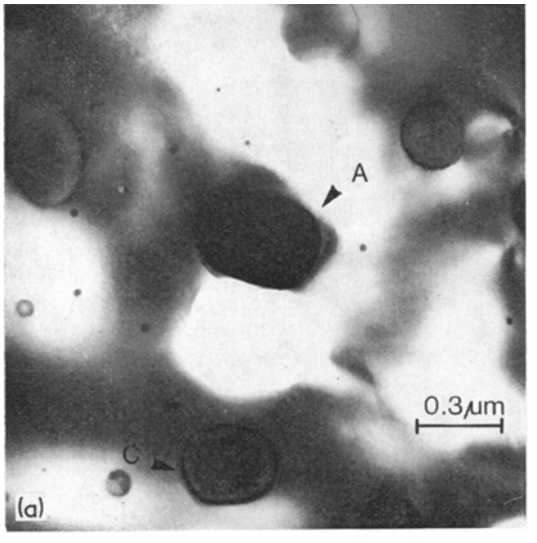

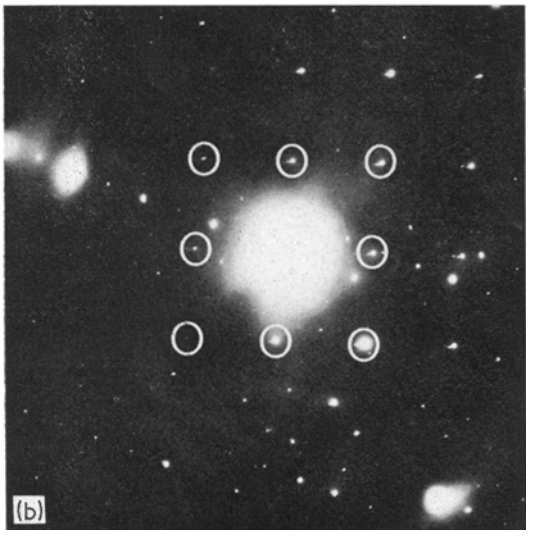

Figure 3 (a) Electron micrograph showing an area of gadolinium iron garnet with a gadolinium orthoferrite inclusion at A. (b) Selected-area electron diffraction pattern from the gadolinium iron garnet matrix and orthoferrite inclusion, orthoferrite diffraction spots ringed. The electron beam is parallel to [111] in the matrix and [001] in the inclusion.

4. Microstructure of gadolinium iron garnet thin films

4.1. Grain growth

A consistent feature of gadolinium iron garnet thin films is the exceedingly high density of inclusions observed in films oxidized at temperatures of greater than 900°C (Fig. 4). In order to study the origin of these inclusions, a series of sintering experiments were made in which films of composition Gd_3Fe_5 were sintered in air for a fixed period of time at successively increasing temperatures. The films were studied in the transmission electron microscope after each sintering treatment. Low temperature sintering studies confirmed the conclusions previously obtained in oxidation studies. At a sintering temperature of 850°C, significant changes began to occur and occasional regions were observed which were greater than 1 μm in extent and gave single crystal selected-area electron diffraction patterns (Fig. 5a). The areas of film surrounding

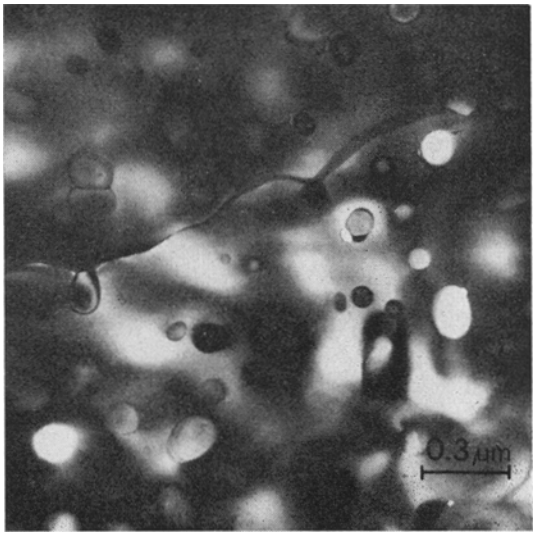

Figure 4 Area of gadolinium iron garnet film produced by oxidation of a film of composition Gd_3Fe_5 for 24 h at 1000°C. The electron beam is parallel to [111].

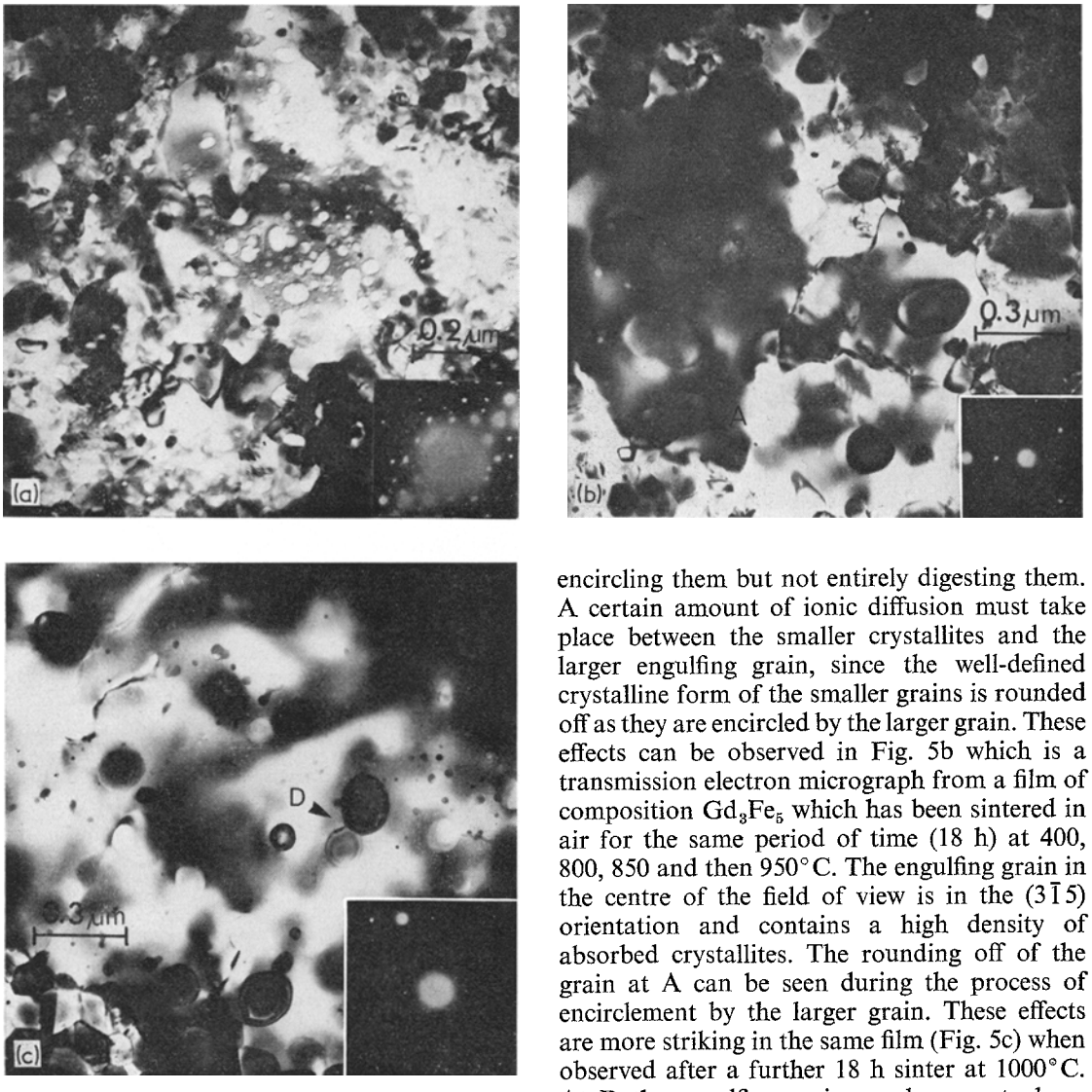

Figure 5 (a) An area of gadolinium iron garnet film produced by sintering a film of composition Gd_3Fe_5 for 18 h at 400, 800 and 850°C. The electron beam is parallel to [1 1 1] for the enlarged grain. (b) An area of the same film after a further sinter at 950°C for 18 h. The electron beam is parallel to [3 $\bar{1}$ $\bar{5}$] for the enlarged grain. (c) An area of the same film after a further sinter at 1000°C for 18 h. The electron beam is close to [1 1 1] for the enlarged grain.

these regions were polycrystalline having grain sizes with an upper limit of approximately 0.2 μm. These single crystal regions appear to form in an unusual manner. The larger single crystal region appears to grow at the expense of the surrounding smaller crystallites by encircling them but not entirely digesting them. A certain amount of ionic diffusion must take place between the smaller crystallites and the larger engulfing grain, since the well-defined crystalline form of the smaller grains is rounded off as they are encircled by the larger grain. These effects can be observed in Fig. 5b which is a transmission electron micrograph from a film of composition Gd_3Fe_5 which has been sintered in air for the same period of time (18 h) at 400, 800, 850 and then 950°C. The engulfing grain in the centre of the field of view is in the (3 $\bar{1}$ 5) orientation and contains a high density of absorbed crystallites. The rounding off of the grain at A can be seen during the process of encirclement by the larger grain. These effects are more striking in the same film (Fig. 5c) when observed after a further 18 h sinter at 1000°C. At D the engulfing grain can be seen to have encircled two grains with the grain boundary between them still intact.

With increase in sintering temperature, those grains which expand preferentially increase in size enveloping further smaller crystallites until the complete film is encompassed. The film then consists of a network of these enveloping grains with the partially consumed smaller grains included within them.

4.2. Inclusion structure

The inclusions of gadolinium iron garnet produced by this process are in general highly misoriented with respect to the surrounding crystal lattice. Occasionally, inclusion orientations

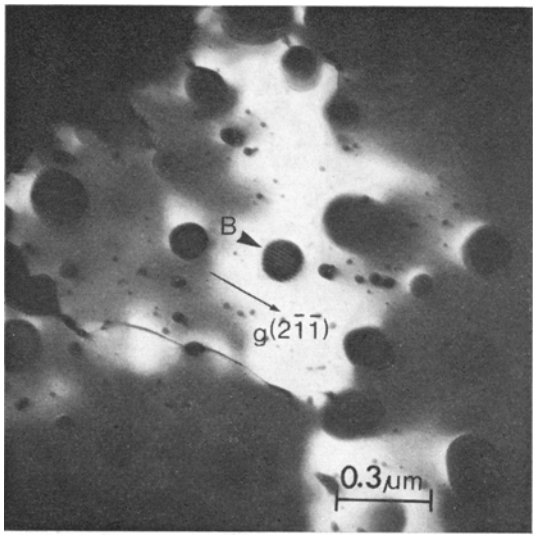

Figure 6 Dark-field micrograph showing a gadolinium iron garnet inclusion, B. The operating reflection is (2$\bar{1}\bar{1}$). The electron beam is parallel to [1$\bar{3}$5] for the inclusion and is parallel to [1$\bar{2}$4] for the matrix.

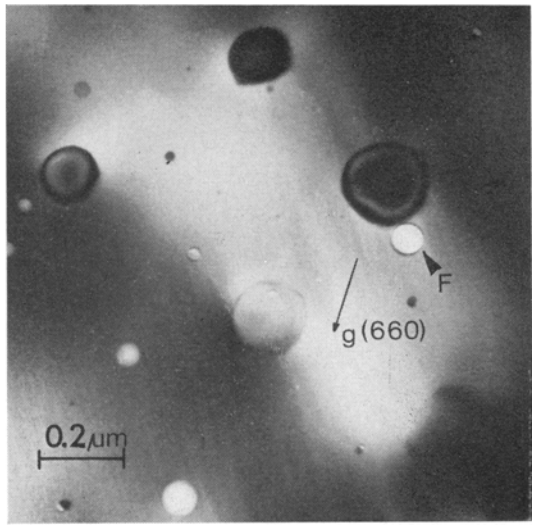

Figure 7 Electron diffraction contrast due to a small spherical pore, F, in gadolinium iron garnet, electron beam parallel to [1 1 1].

are observed which give rise to Moiré fringes. The inclusion B in Fig. 6 exhibiting Moiré fringes has the electron beam perpendicular to the gadolinium iron garnet (1$\bar{3}$5) orientation. The surrounding crystal lattice has the electron beam perpendicular to the (1$\bar{2}$4) orientation. The operating reflection is (2$\bar{1}\bar{1}$) and the (2$\bar{1}\bar{1}$) planes in the inclusion are slightly rotated with respect to the surrounding crystal.

As discussed earlier, not all of the included crystallites encircled by the gadolinium iron garnet grains are misoriented regions of this material. Regions of gadolinium orthoferrite have also been identified (Fig. 3a). Study of the electron diffraction contrast from the inclusions indicates they are lenticular in shape perpendicular to the electron beam since they exhibit thickness fringes (C, Fig. 3a). The majority of the inclusions have a circular cross-section apart from the larger ones which tend to be more irregular and very often consist of a number of grains with intergrain boundaries still intact (D, Fig. 5c).

4.3. Porosity

Accompanying the high density of inclusions formed in gadolinium iron garnet during grain growth are pores which appear to form initially between small oxide crystallites during sintering (Fig. 5a). Observation of the image contrast

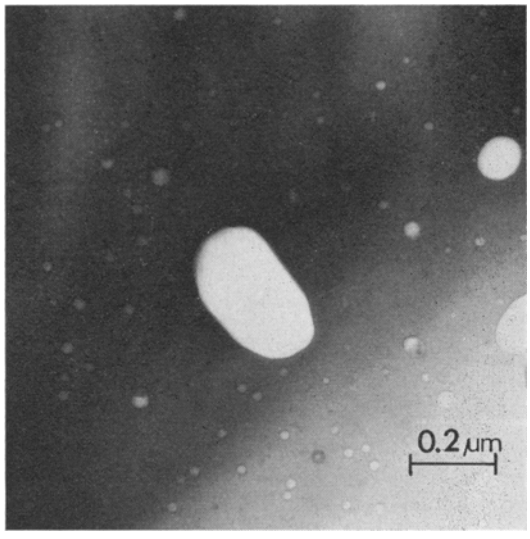

Figure 8 Large pores of irregular shape in gadolinium iron garnet produced by a 36 h oxidation at 1200°C.

confirms that these features are indeed pores giving contrast effects similar to inert gas bubbles in irradiated metals [9]. For small pores and low order reflections no strain contrast can be detected but for higher order reflections faint strain contrast is observed with a line of no contrast perpendicular to the direction of the operating reflection, indicating that these pores are spherical (Fig. 7).

At the temperature where the discontinuous or exaggerated grain growth described above first begins to occur, the pore size is small (Fig. 5a). However, in films which have been further sintered at higher temperatures, larger more irregular pores are observed (Fig. 8) and very often holes are formed.

During the solid state reactions in which iron oxides and gadolinium sesquioxide are converted to the orthoferrite and garnet, oxygen diffusion will be accompanied by diffusion of anion vacancies to the film surface. A large number of these vacancies are likely to be removed by different mechanisms. For example, large numbers of vacancies will be assimilated by existing pores resulting in the observed increase in pore diameter with increased oxidation or sintering temperature.

4.4. Dislocation structure

Another feature observed was occasional grains containing long dislocations with faint contrast (Fig. 9). The dislocations were very often polygonal in character (Fig. 10) and lost contrast over some sections of their length. In some cases strong shade contrast was observed (Fig. 11). The faint image contrast exhibited by these dislocations suggests that the displacements they produce in the lattice are far from perpendicular to the reflecting planes and the loss of contrast along sections of these dislocations which coincide in direction with the operating reflection suggest that they are edge dislocations with Burgers vector contained in planes parallel to the electron beam direction.

To make a thorough investigation of the nature of these dislocations, dark-field microscopy was used and to reduce spherical aberration in the image, the illumination was tilted to ensure the diffracted beam selected for dark-field observations passed along the axis of the objective lens. Two beam conditions were obtained for the selected diffraction spot by slight adjustment of the goniometer stage tilt. Fig. 12 shows two electron micrographs, in different reflection conditions, showing the same area of a gadolinium iron garnet film. Correctly oriented electron diffraction patterns are inset in the corner of each micrograph and the outline of the objective aperture shows the operating reflection for each micrograph. Comparison of the region H in both micrographs indicates that parallel sections of the dislocations present in Fig. 12a, $(0\bar{4}0)$ reflection excited, have lost contrast in Fig. 12b where the (200) reflection is used in dark field. In region J (Fig. 12a), the dislocations are also out of contrast but reappear in Fig. 12b when (200) is excited. Inspection of these micrographs indicates that parts of these long dislocations lose contrast when imaged by a reflection with a parallel or nearly parallel

Figure 9 Electron diffraction contrast from long dislocations in gadolinium iron garnet giving faint contrast. Note dislocation sources at G. The electron beam is parallel to $[2\bar{1}0]$.

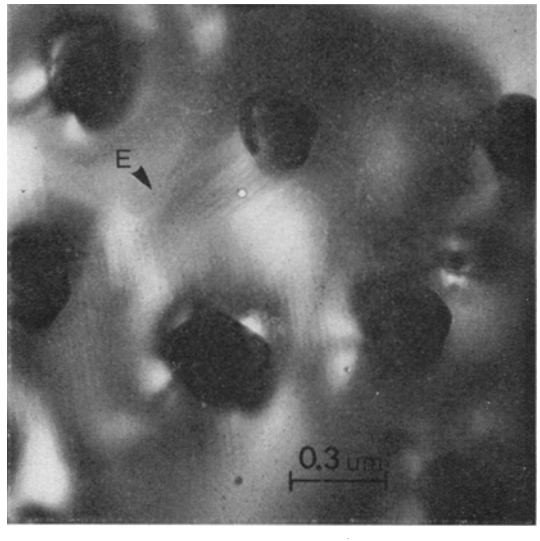

Figure 10 Electron micrograph showing polygonal arrays of dislocations at E.

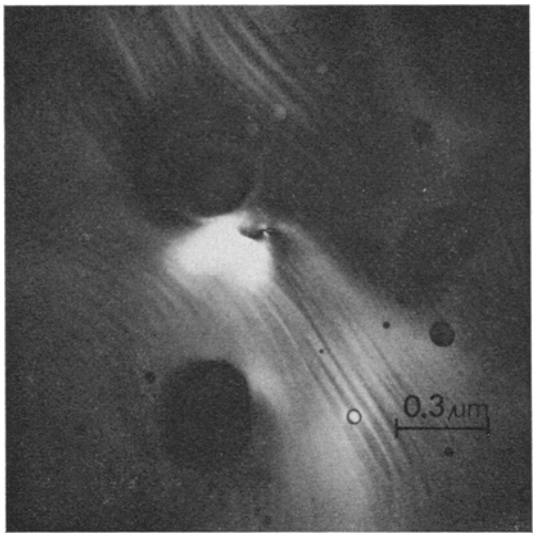

Figure 11 An area of gadolinium iron garnet showing long dislocations in strong contIast. The electron beam is parallel to [001].

diffraction vector. These observations suggest the dislocations are edge dislocations with a Burgers vector perpendicular to the surface of the films so that $\mathbf{g} \cdot \boldsymbol{b} = 0$. The contrast results only from displacements normal to the slip plane and depends upon the factor $\mathbf{g} \cdot \boldsymbol{b}_\wedge \mathbf{u}$ where $\mathbf{u}$ is a unit vector along the dislocation. The contrast expected for an edge dislocation in this situation has been discussed by Howie and Whelan [10] and is greatest for $\mathbf{g} \cdot \mathbf{u} = 0$ and will be zero for $\mathbf{g}$ parallel to $\mathbf{u}$. For $\frac{1}{8}(\mathbf{g} \cdot \mathbf{b}_\wedge \mathbf{u}) \leqslant 0.08$ there is no contrast, corresponding to an angle between $\mathbf{g}$ and $\mathbf{u}$ of less than 10°. The above observations and several observations from other oxidized Gd_3Fe_5 films lead to the conclusion that these dislocations are edge type with Burgers vector perpendicular to (001). Similar arrays of dislocations when observed in other orientations well away from the (001) orientation (Fig. 9) do not lose contrast along sections of their length since the dual conditions for invisibility $\mathbf{g} \cdot \boldsymbol{b} = 0$ and $\mathbf{g} \cdot \boldsymbol{b}_\wedge \mathbf{u} = 0$ are not satisfied.

The strong shade contrast (Fig. 11) discussed above is then due to long range bending associated with these dislocations. The macroscopic bending produced by a single dislocation of this type asymmetrically situated in the film has been discussed previously [10, 11] and it is probable that the strong contrast effects in this particular case are a result of the large number of dislocations involved.

The origin of these dislocations remains to be discussed. The circular arrays of dislocations in Fig. 9 are probably Bardeen-Herring dislocation sources [12] where the dislocations multiply by a process of climb. This type of dislocation source has been observed previously by transmission

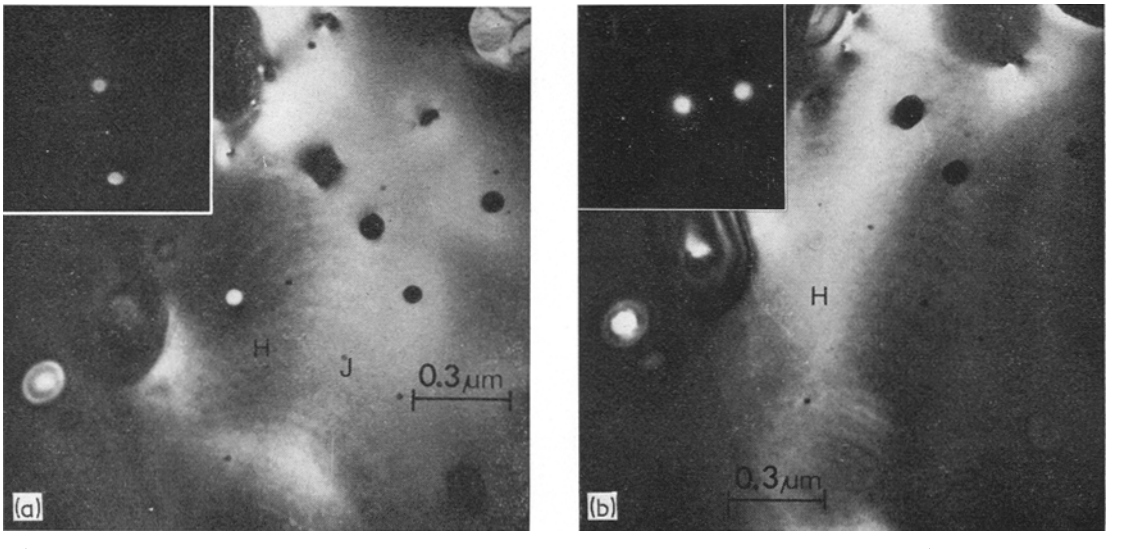

Figure 12 (a) Bright-field electron micrograph showing long dislocations out of contrast at J for sections parallel to the operating diffraction vector (0$\bar{4}$0). The electron beam is parallel to [001]. (b) Dark-field electron micrograph showing long dislocations out of contrast at H for sections parallel to the operating diffraction vector (200).

electron microscopy [13-15]. The role of vacancies in the eventual complete oxidation of the films has been mentioned earlier in connection with pore enlargement as an agent for removal of vacancies. A Bardeen-Herring source is yet another mechanism for removal of the vacancies which are inevitably produced during diffusion between oxide phases. With this source, dislocations multiply by climb absorbing vacancies in the film.

5. Conclusions

Electron diffraction studies of the oxidation of iron and gadolinium thin films agree with the previous investigations of the oxidation of these materials in bulk. For iron thin films the final oxidation product differs but the basic oxidation mechanism still operates. The oxidation of thin composite metal films of composition Gd_3Fe_5 agrees with the results of oxidation of thin films of the individual metals between 300 and 800° C. Above 800° C grains of orthoferrite and garnet form in the film and with increase in oxidation temperature or increase in sintering temperature for previously oxidized films, certain grains with the gadolinium iron garnet structure are observed to expand at the expense of surrounding garnet and orthoferrite grains. Inclusions of garnet and orthoferrite are formed in the film. The garnet films formed in this way contain numerous pores which are observed to increase in size with increase in sintering temperature.

The arrays of long dislocations showing faint contrast are edge dislocations and are believed to be produced by a Bardeen-Herring source. The dislocations multiply by climb absorbing the vacancies generated in the film during the oxidation process.

The abnormal grain growth which has been observed during the formation of these garnet thin films resembles to a limited extent the discontinuous form of grain growth observed in many ceramics. This type of grain growth is believed to occur when inclusions of a second phase, often pores are present in a concentration such that continuous grain growth is no longer possible [16]. Some aspects of the grain growth observed in this investigation are different, the larger growing grains do not completely consume the small neighbouring grains but incorporate them as inclusions which shrink with increased sintering temperature. The events are also complicated by the existence of grains of the orthoferrite phase which are also incorporated as inclusions during grain growth.

Acknowledgements

We wish to thank Professor K. J. Standley for encouraging this research project and also the Science Research Council for a research grant B/SR/9281 for investigation of the growth and physical properties of ferrimagnetic thin films.

References

1. E. SAWATSKY and E. KAY, *J. Appl. Phys.* **42** (1971) 367.
2. J. E. MEE, G. R. PULLIAM, J. L. ARCHER and P. J. BESSER, *IEEE Trans. Magnetics*, **Mag-5** (1969) 717.
3. R. J. GAMBINO, *J. Appl. Phys.* **38** (1967) 1129.
4. E. BANKS, N. H. RIEDERMANN, H. W. SCHLEUNING and L. M. SILBER, *ibid* **32** (1961) 44S.
5. R. ENGIN and A. G. FITZGERALD, *J. Mater. Sci.* **8** (1973) 169.
6. K. HAUFFE, "Oxidation of Metals" (Plenum Press, New York, 1965).
7. O. KUBASCHEVSKY and B. E. HOPKINS, "Oxidation of Metals and Alloys" (Butterworths, London, 1967).
8. N. D. GREENE and F. G. HODGE, *Corrosion* **22** (1966) 206.
9. L. M. BROWN and D. J. MAZEY, *Phil. Mag.* **8** (1964) 1081.
10. A. HOWIE and M. J. WHELAN, *Proc. Roy. Soc. (London)* **A267** (1962) 206.
11. M. WILKENS, M. RUHLE and F. HAUSSERMAN, *Phys. Stat. Sol.* **22** (1967) 689.
12. J. BARDEEN and C. HERRING, in "Imperfections in nearly perfect crystals", edited by W. Shockley, J. H. Holloman, R. Maurer and F. Seitz (Wiley, New York, 1952).
13. K. H. WESTMACOTT, R. S. BARNES and R. E. SMALLMAN, *Phil. Mag.* **7** (1962) 1585.
14. J. D. EMBURY and R. B. NICHOLSON, *Acta Metallurgica* **11** (1963) 347.
15. O. N. SRIVASTAVA and J. SILCOX, *Phil. Mag.* **18** (1963) 503.
16. W. D. KINGERY, "Introduction to Ceramics" (Wiley, New York, 1960).

Received 3 July and accepted 26 September 1973.